Metabolic reprogramming of human CD8+ memory T cells through loss of SIRT1

Mark Y. Jeng,[1,2]* Philip A. Hull,[1,5]* Mingjian Fei,[1,2] Hye-Sook Kwon,[1,2] Chia-Lin Tsou,[1] Herb Kasler,[1,4] Che-Ping Ng,[1,4] David E. Gordon,[1,3] Jeffrey Johnson,[1,3] Nevan Krogan,[1,3] Eric Verdin,[1,4] and Melanie Ott[1,2]

[1]Gladstone Institutes, San Francisco, CA
[2]Department of Medicine and [3]Quantitative Biology Institute, Department of Cellular and Molecular Pharmacology, University of California, San Francisco, San Francisco, CA
[4]The Buck Institute for Research on Aging, Novato, CA
[5]Westfälische Wilhelms-Universität Münster, Münster, Germany

The expansion of CD8+CD28− T cells, a population of terminally differentiated memory T cells, is one of the most consistent immunological changes in humans during aging. CD8+CD28− T cells are highly cytotoxic, and their frequency is linked to many age-related diseases. As they do not accumulate in mice, many of the molecular mechanisms regulating their fate and function remain unclear. In this paper, we find that human CD8+CD28− T cells, under resting conditions, have an enhanced capacity to use glycolysis, a function linked to decreased expression of the NAD+-dependent protein deacetylase SIRT1. Global gene expression profiling identified the transcription factor FoxO1 as a SIRT1 target involved in transcriptional reprogramming of CD8+CD28− T cells. FoxO1 is proteasomally degraded in SIRT1-deficient CD8+CD28− T cells, and inhibiting its activity in resting CD8+CD28+ T cells enhanced glycolytic capacity and granzyme B production as in CD8+CD28− T cells. These data identify the evolutionarily conserved SIRT1–FoxO1 axis as a regulator of resting CD8+ memory T cell metabolism and activity in humans.

INTRODUCTION

The loss of the T cell coreceptor CD28 is a prominent hallmark of immune aging. In umbilical cord blood, virtually all CD8+ T cells express CD28 (Azuma et al., 1993). However, with repeated exposure to antigens over the course of an individual's life, a majority of CD8+ T cells in human peripheral blood will become progressively differentiated and eventually lose CD28 surface expression (Effros et al., 1994; Posnett et al., 1994; Fagnoni et al., 1996). This process is accelerated in response to persistent viral infections, such as CMV and HIV (Saukkonen et al., 1993; Dutra et al., 1996; Effros, 2005; Wertheimer et al., 2014). Functionally, CD8+CD28− T cells have an impaired proliferative response to antigen-specific activation, but they remain very cytotoxic, acquiring high expression of natural killer cell receptors and producing greater levels of effector molecules, such as granzyme B (GZMB), perforin (PRF1), and IFN-γ, under resting and activated conditions (Tarazona et al., 2001; Weng et al., 2009). Given the ubiquitous presence of CD8+CD28− T cells and their connection to aging, a better understanding of the molecular mechanisms driving their uncontrolled production of effector molecules is needed.

Human sirtuins (SIRT1–7) are highly conserved proteins that regulate cellular processes linked to metabolism and organismal longevity (Guarente, 2011; Houtkooper et al., 2012).

Enhancing the expression of the ancestral SIR2 protein in yeast and worms promotes organismal life span extension (Kaeberlein et al., 1999; Tissenbaum and Guarente, 2001). Silent mating type information regulation 2 homologue 1 (SIRT1), the closest mammalian homologue of SIR2, is a nuclear nicotinamide adenine dinucleotide (NAD+)–dependent protein deacetylase that targets many transcription factors involved in different cellular processes (Chang and Guarente, 2014). SIRT1 levels decrease with age in the brain, liver, skeletal muscle, and white adipose tissue of rodents, possibly contributing to the aging processes in these tissues (Quintas et al., 2012; Gong et al., 2014; Cho et al., 2015). Conditions that activate SIRT1 activity (e.g., treatment with the phytoalexin resveratrol [RSV]) improve symptoms associated with metabolic dysfunction and protect against age-related diseases, such as cancer, neurodegeneration, and cardiovascular disease (Jin et al., 2008; Tanno et al., 2010; Hall et al., 2013). Similarly, boosting SIRT1 activity with the NAD+ precursor nicotinamide riboside in aged mice results in improved mitochondrial and stem cell function and a modest life span extension (Cantó et al., 2012; Zhang et al., 2016). Although several fate-determining functions of SIRT1 have emerged in regulatory, proinflammatory, and anergic CD4+ and activated CD8+ effector T cells (van Loosdregt et al., 2010;

*M.Y. Jeng and P.A. Hull contributed equally to this paper.

Correspondence to Melanie Ott: mott@gladstone.ucsf.edu

Beier et al., 2011; Kuroda et al., 2011; Kwon et al., 2012; Lim et al., 2015), its role in CD8$^+$ memory T cells remains unknown.

Here, we show that SIRT1 expression is markedly down-regulated in terminally differentiated CD8$^+$CD28$^-$ memory T cells, a population that accumulates during human aging (Fagnoni et al., 1996). Loss of SIRT1 and enhanced proteasomal degradation of the downstream transcription factor forkhead box protein O1 (FoxO1) promote an enhanced glycolytic capacity and increased GZMB secretion under resting conditions, pointing to the SIRT1–FoxO1 axis as an important mechanism for preserving resting memory T cell metabolism and function.

RESULTS AND DISCUSSION
Down-regulation of SIRT1 in CD8$^+$CD28$^-$ T cells
Given the known roles of SIRT1 in organismal aging and T cell function, we examined SIRT1 expression in human CD8$^+$CD28$^-$ T cells. We found SIRT1 protein expression markedly down-regulated in freshly isolated, nonactivated CD8$^+$CD28$^-$ T cell populations when compared with naive or CD28$^+$ memory T cells (Fig. 1, A and B). Of note, we found the percentage of effector T cells in the CD28$^-$ population to be <5% as previously described (Amara et al., 2004; Miller et al., 2008). Reduced SIRT1 levels were consistent across samples from multiple individuals (Fig. 1 C). *SIRT1* mRNA levels were not significantly different (Fig. 1 D), implying that *SIRT1* transcription was not affected. Importantly, expression of other nuclear sirtuins, SIRT6 and SIRT7, was unchanged in CD8$^+$CD28$^-$ T cells (Fig. 1 E).

To test whether the down-regulation of SIRT1 is causally linked to the loss of CD28 coreceptor expression, we performed a long-term culture of sorted CD8$^+$CD28$^+$ T cells (99.9% purity) in the presence of IL-15, a memory T cell survival and proliferation cytokine, which led to a significant loss of CD28 surface expression (Fig. 1, F and G; Chiu et al., 2006). When CD8$^+$CD28$^+$ and CD8$^+$CD28$^-$ T cells were resorted after 20 d of culture, we observed no differences in SIRT1 expression, indicating that the down-regulation of SIRT1 was specific to blood-derived CD8$^+$CD28$^-$ T cells and not causally related to loss of CD28 (Fig. 1 H).

Loss of SIRT1 correlates with metabolic reprogramming
Metabolism is a key driver of T cell function. Although naive and resting memory T cells depend primarily on mitochondrial oxidative phosphorylation and fatty acid oxidation, activated T cells rapidly shift their metabolism toward aerobic glycolysis to support their full effector function (Pearce et al., 2013). Because SIRT1 regulates mitochondrial function in skeletal muscle (Sack and Finkel, 2012), and defective mitochondrial function has been reported in senescent terminally differentiated RA$^+$ effector memory T cells (T$_{EMRA}$ cells; Henson et al., 2014), we investigated whether low SIRT1 expression changed the metabolism of T cells. Using Seahorse technology, we first measured the oxygen consumption rate (OCR) in naive, CD28$^+$, and CD28$^-$ human CD8$^+$ memory T cells with a standard mitochondrial stress test, which included treatments with oligomycin (an inhibitor of ATP synthase), carbonyl cyanide 4-(trifluoromethoxy)phenylhydrazone (FCCP; an uncoupling agent), and a combination of antimycin A and rotenone (inhibitors of complex III and complex I, respectively). We found no difference in OCR between resting CD8$^+$ naive, CD28$^+$, and CD28$^-$ T cells with or without the addition of the mitochondrial toxins (Fig. 2 A), indicating that mitochondrial oxygen consumption was undisturbed in T cells with low SIRT1 expression.
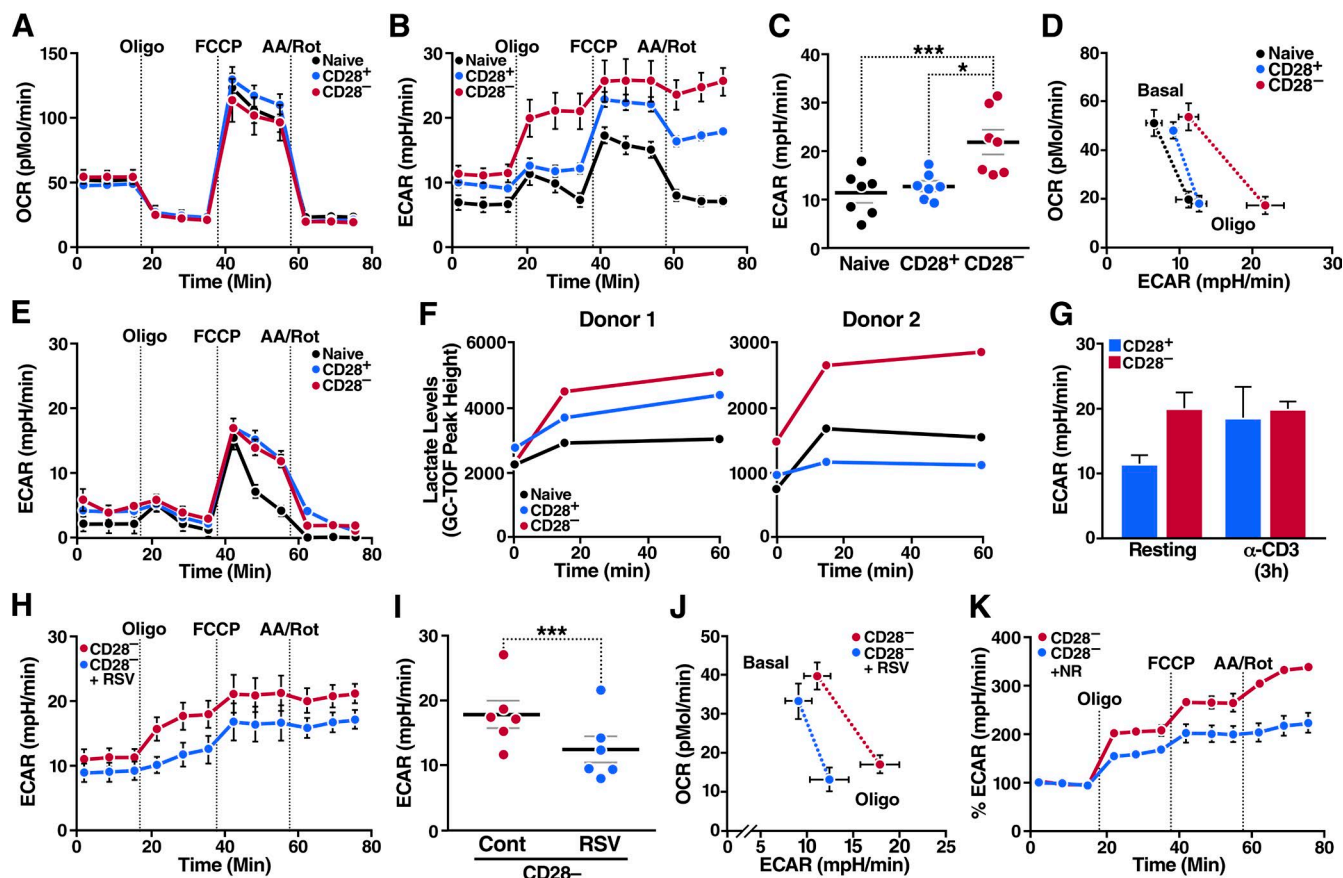
Figure 2. Loss of SIRT1 promotes metabolic reprogramming in resting CD8+CD28− T cells. Metabolism of sorted human CD8+ T cell populations was assessed using an extracellular flux (XF) analyzer. (A and B) OCR and ECAR measured in freshly isolated T cell subsets (shown is the mean of biological replicates, $n = 7$). (C) Glycolytic capacity of T cell subsets ($n = 7$, paired one-way ANOVA). (D) Energy profile (OCR vs. ECAR) of sorted T cells. Dotted lines indicate corresponding OCR-ECAR data points (shown is the mean of biological replicates, $n = 7$). (E) ECAR measurement after 48 h of glucose deprivation (representative, $n = 2$). (F) Lactate concentrations in sorted T cell populations were analyzed by gas chromatography time-of-flight mass spectrometry (GC-TOF) after oligomycin treatment ($n = 2$). (G) Glycolytic capacity of activated and resting T cells ($n = 2$ biological and 6 technical replicates). (H) ECAR of CD8+CD28− T cells treated with 50 µM RSV for 48 h (shown is the mean of biological replicates, $n = 7$). (I) Glycolytic capacity of RSV-treated CD8+CD28− T cells ($n = 6$, paired two-tailed Student's t test). (J) Energy profile (OCR vs. ECAR) of RSV-treated CD8+CD28− T cells (shown is the mean of biological replicates, $n = 7$). (K) ECAR of CD8+CD28− T cells treated with nicotinamide riboside for 48 h (representative normalized to 100% baseline, $n = 2$). Data are mean ± SEM of individual donors. *, $P < 0.05$; ***, $P < 0.001$. AA/Rot, antimycin A/rotenone; mpH/min, milli-pH units per minute.

In contrast, CD8+CD28− T cells exhibited a distinctive glycolytic profile, highlighted by their markedly elevated extracellular acidification rate (ECAR) after exposure to oligomycin (Fig. 2 B). The ECAR response to oligomycin, called glycolytic capacity, measures how well cells are primed to use glycolysis when ATP production from oxidative phosphorylation is impaired. One function of this capacity is to support the glycolytic gene program in CD8+ effector memory T cells (T$_{EM}$ cells) immediately after activation (Gubser et al., 2013). In resting CD8+CD28− T cells, we found that the glycolytic capacity (maximum ECAR after oligomycin injection) was consistently increased among various donors (Fig. 2 C), producing a unique energy profile (OCR vs. ECAR plot) defined by a characteristic shift in ECAR, but not OCR, in response to oligomycin (Fig. 2 D). This increased glycolytic

capacity depended on the presence of extracellular glucose (Fig. 2 E and Fig. S1 A) and was accompanied by increased levels of lactate, as expected (Fig. 2 F). A consistent increase in glycolytic capacity in CD28− over CD28+ memory T cells was unique to the resting state and was not observed after activation with CD3 antibodies when CD28+ T cells increased their glycolytic activities to the same level as CD28− T cells (Fig. 2 G and Fig. S1, B and C).

To determine whether low SIRT1 levels and high glycolytic capacity were linked in CD8+CD28− T cells, we treated resting cells with RSV to enhance SIRT1 activity (Hubbard et al., 2013). With little toxicity (Fig. S1 D), RSV lowered the glycolytic capacity (Fig. 2, H and I; and Fig. S1 E) and shifted the energy profile (Fig. 2 J) of CD8+CD28− T cells closer to levels in CD8+ naive and CD28+ memory T

cells. Similar results were obtained after treatment with the NAD$^+$ precursor nicotinamide riboside, independently linking the control of glycolytic capacity to SIRT1 activity in CD8$^+$CD28$^-$ T cells (Fig. 2 K).

Altered FoxO1 target gene expression in CD8$^+$CD28$^-$ T cells

Because the switch to a glycolytic program in activated T cells is associated with extensive changes in gene expression (Man and Kallies, 2015), we performed microarray analysis to define the global gene expression profiles of resting CD8$^+$CD28$^+$ and CD28$^-$ T cells isolated from three individual blood donors. This analysis revealed differential regulation of 159 genes within resting CD8$^+$CD28$^-$ T cells (log$_2$ fold change ≥1.0; false discovery rate [FDR] ≤0.05). Down-regulated genes included *CD28* and previously reported T cell homing receptors, such as *C-C chemokine receptor type 7* (*CCR7*) and L-selectin (*CD62L*), as well as long-term survival cytokine receptor *IL7R* (Fig. 3 A and Table S1; Hamann et al., 1997; Sallusto et al., 1999; Joshi et al., 2007). Several natural killer receptors, including *killer cell lectin-like receptor G1* (*KLRG1*), and cytolytic granzymes were up-regulated (Henson et al., 2009). Supporting previous studies (Fann et al., 2005; Sun et al., 2008; Chen et al., 2013), we found that under non-activated conditions, terminally differentiated CD8$^+$CD28$^-$ T cells expressed markedly higher *GZMB* mRNA and intracellular GZMB protein levels (Fig. S2, A and B). *PRF1* and *IFNG* transcripts were also increased (Fig. S2 A).

Using ingenuity pathway analysis (IPA), we generated a list of upstream transcription factors (ordered from most to least significant p-value) that were predicted to regulate the variable gene expression between the two populations (Fig. 3 A). The top candidate was FoxO1 (P = 2.97 × 10^{-6}), a SIRT1 substrate implicated in regulating multiple metabolic pathways in other cell types (Gross et al., 2008). FoxO1 also binds and regulates the expression of multiple genes that control T cell homing, homeostasis, tolerance, and memory differentiation (Ouyang et al., 2009; Rao et al., 2012; Kim et al., 2013; Staron et al., 2014), and the FoxO homologue DAF-16 is a substrate of SIRT1 in *Caenorhabditis elegans* aging (Lin et al., 1997; Berdichevsky et al., 2006).

With quantitative RT-PCR (qRT-PCR) and flow cytometry, we verified the down-regulation of canonical FoxO1 target genes in CD8$^+$CD28$^-$ T cells, including lymph node–homing receptors *CCR7* and *CD62L* and the growth factor *IL7 receptor* (*IL7R*; Kerdiles et al., 2009). CD8$^+$CD28$^-$ T cells also expressed increased *KLRG1*, a marker of terminal T cell differentiation that is inversely related to FoxO1 expression in CD8$^+$ T cells (Fig. 3, B and C; Michelini et al., 2013).

SIRT1 regulates FoxO1 protein expression in CD8$^+$ T cells

FoxO proteins are targets of the deacetylase function of SIRT1 (Brunet et al., 2004; Motta et al., 2004). We confirmed that this is also the case with FoxO1 in CD8$^+$ T cells by performing mass spectrometry on freshly isolated T cells treated with the SIRT1 inhibitor 6-chloro-2,3,4,9-

tetrahydro-1H-carbazole-1-carboxamide (Ex–527) and histone deacetylase inhibitor trichostatin A (TSA). The latter inhibitor was used to increase overall acetylation levels. We identified 831 acetylated lysine-containing peptides, among them Lys262-acetylated FoxO1, a site that regulates DNA binding of FoxO1 in human liver carcinoma cells (Matsuzaki et al., 2005). Lys262-acetylated FoxO1 was 10 times more abundant in T cells treated with TSA and Ex–527 than in cells treated with TSA alone, indicating that it is a specific SIRT1 target site in CD8$^+$ T cells (Fig. S2 C). FoxO1 hyperacetylation in response to SIRT1 inhibition is linked to enhanced FoxO1 degradation via protein kinase B (PKB/Akt)–mediated phosphorylation, as it attenuates the DNA-binding affinity of FoxO1 and facilitates its nuclear export and degradation (Daitoku et al., 2004; Frescas et al., 2005). Accordingly, FoxO1 protein levels were decreased in both nuclear and cytoplasmic compartments of CD8$^+$CD28$^-$ T cells (Fig. 3 D). Down-regulation of FoxO1 was consistently observed among different donors and exhibited a pattern of gradual decline in protein expression similar to SIRT1 from naive > CD28$^+$ > CD28$^-$ T cell populations (Fig. 1, B and C; and Fig. 3 E). No significant differences in *FoxO1* mRNA levels were observed, supporting that FoxO1, like SIRT1, is posttranscriptionally down-regulated in CD8$^+$CD28$^-$ T cells (Fig. 3 F). Indeed, treatment with proteasome inhibitor MG132 rescued protein expression of FoxO1 in CD8$^+$CD28$^-$ T cells to approximately half of its levels in CD28$^+$ T cells (Fig. 3, G and H), supporting the model that FoxO1 is proteasomally degraded in the absence of SIRT1. In contrast, SIRT1 levels did not respond to MG132 treatment, implicating that expression of FoxO1 and SIRT1 proteins is distinctly regulated in CD8$^+$CD28$^-$ T cells.

We also examined SIRT1 and FoxO1 protein levels in sorted CD8$^+$ memory T cell subsets using CCR7 and CD45RA as additional differentiation markers (Fig. S2 D). We found a progressive down-regulation of both proteins in CD28$^+$ central memory (T$_{CM}$) and transitional memory (T$_{TM}$) T cells, mirroring the progressive loss of the FoxO1 target CCR7 in these cells (Fig. S2, D–G). Both proteins were most down-regulated in the T$_{EM}$ and T$_{EM}$/T$_{EMRA}$ populations identified in CD8$^+$CD28$^-$ T cells, with no difference detected between T$_{EM}$ and T$_{EMRA}$ populations (Fig. S2, D–G). The same was observed when intracellular staining for FoxO1 was performed in unsorted cells, and no difference was observed between cells isolated from CMV$^+$ or CMV$^-$ donors (Fig. S2 H). Throughout all cell subsets, SIRT1 and FoxO1 proteins levels were strongly correlated (R^2 = 0.8197), supporting the model that SIRT1 and FoxO1 protein levels are linked in human CD8$^+$ memory T cells (Fig. S2 I).

To confirm that SIRT1 acts upstream of FoxO1, we performed clustered regularly interspaced short palindromic repeat (CRISPR) editing of the *SIRT1* gene in CD8$^+$ T cells using nucleofection of purified CRISPR–associated protein 9 (Cas9) ribonucleoprotein (RNP) complexes containing guide RNAs specific for SIRT1. This method is highly effi-
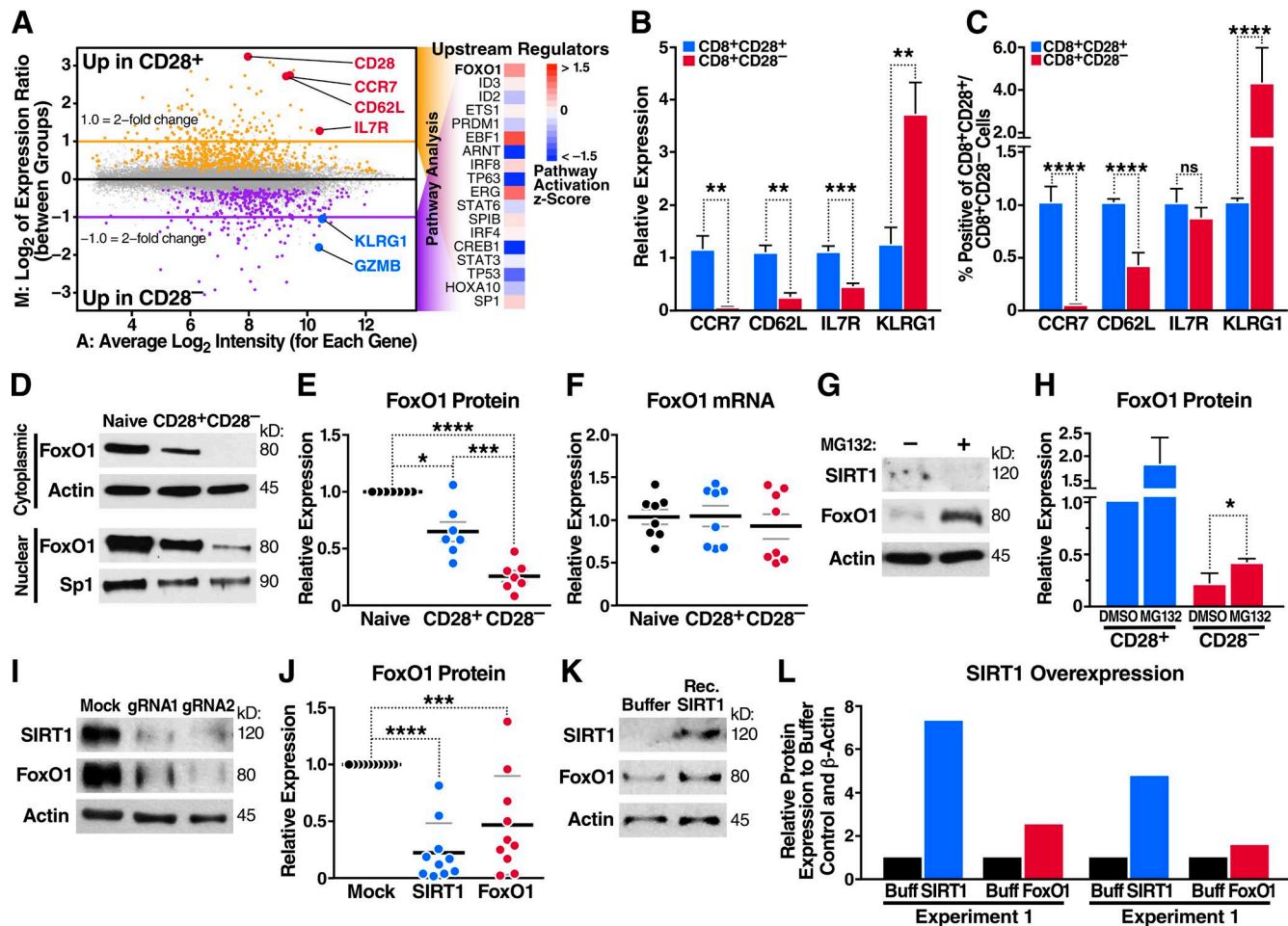
Figure 3. **Altered FoxO1 gene expression in CD8⁺CD28⁻ T cells.** (A) Microarray analysis in CD8⁺CD28⁺ and CD28⁻ T cells, predicting FoxO1 as an altered transcriptional regulator in CD8⁺CD28⁻ T cells. (B) *CCR7*, *CD62L*, *IL7R*, and *KLRG1* mRNA were assessed by qRT-PCR and normalized to *RPL13A* mRNA from sorted human T cell populations ($n = 5$, paired one-way ANOVA). (C) Peripheral blood mononuclear cells were stained for CD3, CD8, CD28, and indicated markers as in B and analyzed by flow cytometry ($n = 5$, paired one-way ANOVA). (D and E) FoxO1 expression in sorted human T cells was measured by Western blot (representative, $n = 7$, paired two-tailed Student's *t* test). (F) *FoxO1* mRNA was analyzed by qRT-PCR and normalized to *RPL13A* ($n = 8$). (G and H) CD28⁺ and CD28⁻ T cells were treated with 20 µM MG132 for 6 h, and FoxO1 expression was measured by Western blot ($n = 3$, unpaired two-tailed Student's *t* test, G shows CD28⁻ T cells). (I and J) SIRT1 knockdown by Cas9–RNP nucleofection and Western blot for SIRT1 and FoxO1 expression ($n = 9$, two-way ANOVA). (K) Nucleofection of recombinant SIRT1 protein into CD8⁺ T cells and Western blot for SIRT1 and FoxO1 protein 18 h after nucleofection (representative, $n = 2$). (L) Densitometry of two independent experiments ($n = 2$). Data are mean ± SEM of individual donors. *, $P < 0.05$; **, $P < 0.01$; ***, $P < 0.001$; ****, $P < 0.000$. ns, not significant.

cient in primary human T cells and was used in CD4⁺ T cells for host factor gene editing in HIV infection (Schumann et al., 2015; Hultquist et al., 2016; Park et al., 2017). When SIRT1 protein expression was efficiently decreased with two independent guide RNAs, FoxO1 levels were reproducibly decreased (Fig. 3, I and J). Conversely, SIRT1 overexpression using T cell nucleofection with recombinant SIRT1 protein led to a modest but consistent increase in FoxO1 levels as early as 18 h after nucleofection (Fig. 3, K and L). These data support the model that SIRT1 expressed in human CD8⁺ memory T cells stabilizes FoxO1 protein levels.

Inhibition of FoxO1 reprograms T cell metabolism and cytotoxicity

To determine whether FoxO1 is the downstream target of SIRT1, thereby preventing increases in glycolytic capacity and cytotoxic activity in resting CD8⁺ memory T cells, we treated resting CD8⁺ naive or CD28⁺ memory T cells with the compound AS1842856. AS1842856 blocks FoxO1 transcriptional activity by selectively binding its dephosphorylated active form (Nagashima et al., 2010). Inhibiting FoxO1 with AS1842856 consistently enhanced the glycolytic capacity (Fig. 4 A) and shifted the energy profile (Fig. 4 B) in
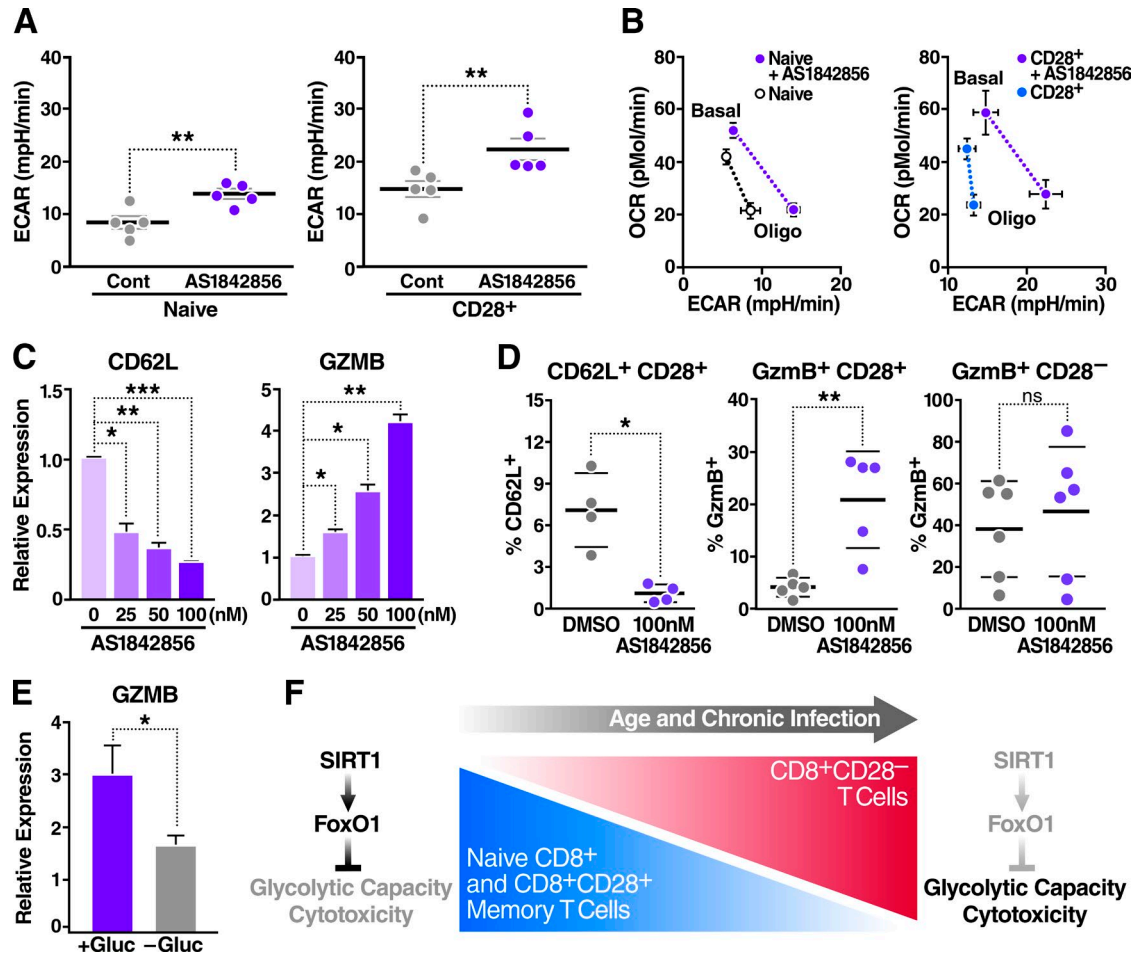
Figure 4. **FoxO1 inhibition reprograms CD8+ T cell metabolism and induces cytotoxicity.** Metabolism of sorted human CD8+ T cell populations was assessed using an extracellular flux analyzer. (A) Glycolytic capacity of sorted human T cell populations treated with 100 nM AS1842856 for 48 h ($n = 5$, paired two-tailed Student's t test). (B) Energy profile (OCR vs. ECAR) of T cell subsets treated as in A (shown is the mean of biological replicates, $n = 5$). (C) Gene expression was measured by qRT-PCR, normalized to RPL13A mRNA, and relative to untreated human CD8+ T cells with increasing doses of AS1842856 for 48 h ($n = 3$, paired two-tailed Student's t test). (D) Surface marker analysis by flow cytometry after 72 h of incubation with 100 nM AS1842856 ($n = 5$, two-way ANOVA). (E) Gene expression after CD8+ T cell treatment with 100 nM AS1842856 $\pm$ glucose for 48 h, measured by qRT-PCR, and normalized to *RPL13A* mRNA and to untreated cells ($n = 5$, paired two-tailed Student's t test). Data are mean $\pm$ SEM of individual donors. *, $P < 0.05$; **, $P < 0.01$; ***, $P < 0.001$; mpH/min, milli-pH units per minute. (F) Model: a dynamic SIRT1–FoxO1 axis regulates metabolism and cytotoxicity in CD8+ T cells. This axis is lost in CD8+CD28− T cells, resulting in increased T cell glycolytic capacity and cytotoxicity.

both cell populations, replicating the phenotype observed in CD8+CD28− T cells with reduced FoxO1 expression.

AS1842856 had no effect on cell viability (Fig. S3 A) and, as expected, suppressed expression of the FoxO1 target genes *CD62L* and *IL7R* in resting human CD8+ T cells (Fig. 4 C and Fig. S3 B). In contrast, AS1842856 significantly and dose-dependently increased basal *GZMB* mRNA and intracellular protein levels in CD8+CD28+, but not in CD8+CD28−, T cells, supporting the model that metabolic and cytotoxic characteristics of CD8+CD28− T cells are linked via FoxO1 (Fig. 4, C and D; and Fig. S3 C). Treatment with AS1842856 did not cause T cell activation (Fig. S3 D), but required glucose consumption (Fig. 4 E) as reported by others (Cham et al., 2008; Chang et al., 2013), further

linking glycolytic and cytotoxic capacities of CD8+ T cells under resting conditions.

Collectively, we identify the SIRT1–FoxO1 axis as a novel regulator of metabolic reprogramming in human CD8+ T cells as they first progress from naive T cells to CD28+ central and transitional memory cells, and ultimately to CD28− T_{EM} and T_{EMRA} cells. The accumulation of these terminally differentiated CD8+CD28− T cells is a consistent immunological change in aging humans (Fagnoni et al., 1996). Although these cells are a product of repeated antigen stimulation and have been linked to pathology because of their uncontrolled production of effector molecules (Vallejo, 2005; Weng et al., 2009), our molecular and metabolic understanding of how CD28− T cells differ from their naive and

CD28^{+} memory T cell counterparts and of their causal link to aging is still limited.

We propose a model in which reduced levels of SIRT1 destabilize the expression and function of FoxO1 to enhance the glycolytic and cytotoxic (i.e., GZMB producing) capacities of resting CD8^{+}CD28^{−} T cells, thereby contributing to immune dysfunctions observed in this cell type (Fig. 4 F). Beyond its well-characterized role of inducing apoptosis in virally infected cells, continuously circulating GZMB degrades extracellular matrix proteins and propagates inflammatory signaling, thus possibly playing a pathophysiological role in age-related chronic inflammatory diseases (Darrah and Rosen, 2010; Hiebert and Granville, 2012).

We show that SIRT1 levels diminish with increased T cell differentiation status and find a strong correlation with FoxO1 expression in human CD8^{+} T cells, thereby adding new insights into the regulation of FoxO1-mediated lineage determination and metabolic reprogramming (Kerdiles et al., 2010; Gubser et al., 2013; Michelini et al., 2013). FoxO1 is known to control *GZMB* transcription through the repression of the transcription factor T box transcription factor 21 (T-bet) before antigen stimulation (Rao et al., 2012). We extend these findings by linking them to the upstream regulatory role of SIRT1 and the metabolic state of resting CD8^{+} T cells.

Although this represents a new role for the SIRT1–FoxO1 axis in human CD8^{+} T cells, previous studies have found this axis to be involved in regulating other cellular processes, such as maintenance and growth of skeletal muscle (Lee and Goldberg, 2013), apoptosis in senescent cardiomyocytes (Sin et al., 2014), intracellular signaling in tissues (Gross et al., 2008; Sin et al., 2015), and regulating the hippocampal homeostasis in aging mice (Jenwitheesuk et al., 2017). In *C. elegans,* the homologous SIR2–DAF-16–FOXO pathway, when strengthened, extends organismal life span (Tissenbaum and Guarente, 2001).

Our new findings now connect this evolutionarily conserved pathway with T cell metabolism and cytotoxicity. Strengthening the SIRT1–FoxO1 axis may provide a potential therapeutic intervention to reprogram terminally differentiated memory T cells and delay the immune aging process (Guarente, 2011; Houtkooper et al., 2012; Zhang et al., 2016).

MATERIALS AND METHODS
Human donors and T cell population sorting
Blood samples were collected at the Blood Centers of the Pacific in San Francisco, CA. All donors were kept anonymous and provided written informed consent. Total human CD8^{+} T cells were enriched via negative selection using the RosetteSep human CD8^{+} T cell enrichment cocktail (15063; Stemcell). The following antibodies were used to stain peripheral blood mononuclear cells or enriched CD8^{+} naive, CD8^{+}CD28^{+} memory, and CD8^{+}CD28^{−} T cells: CD3-PECy5 (555334; BD Biosciences) and CD3-APC-H7 (560176; BD Biosciences), CD8-V450 (560347; BD Biosciences), CD28-PE (12–0289; eBioscience), CD45RA-APC

(17–0458; eBioscience), and CCR7-PECy7 (557648; BD Biosciences). Flow cytometry was performed on an LSRII or Calibur DxP8 flow cytometer (both BD Biosciences) and was analyzed with FlowJo software. Sorting was performed on an ARIA II (BD Biosciences).

Intracellular flow
CD8^{+} T cells were cultured for 1 h in complete RPMI in the presence of brefeldin A and subsequently stained for viability using the viability dyes eFluor 506, 520, or 780 (eBioscience), according to the provided protocol. After surface marker staining, cells were permeabilized and fixed using the Foxp3/Transcription Factor Fixation/Permeabilization Concentrate and Diluent kit (eBioscience). Intracellular GZMB-FITC (515403; BioLegend), FoxO1-PE (14262; Cell Signaling Technology), and isotope control (5742; Cell Signaling Technology) staining was performed in FOXP3 perm/wash buffer for 1 h at 4°C. After washing and fixation of the cells in 1% paraformaldehyde/PBS, cells were analyzed by flow cytometry.

T cell culture and treatment conditions
T cells were cultured in RPMI 1640 medium supplemented with 10% FBS, 2 mM L–glutamine, and penicillin–streptomycin. RSV (R5010; Sigma-Aldrich) was used at 25 or 50 µM for 48 h. FoxO1 inhibitor AS1842856 (344355; Calbiochem) was used at 25, 50, or 100 nM for 48 h. MG132 (M7449; Sigma-Aldrich) was used at 20 µM for 6 h. Nicotinamide riboside was obtained from A.A. Sauve's lab (Weill Cornell Medical College, New York, NY) and used at 0.5 or 1 µM for 48 h.

T cell transduction using CRISPR Cas9–RNP nucleofection
CD8^{+} T cells, enriched as described under the Human donors and T cell population sorting section, were activated with plate-bound anti-CD3 (10 µg/ml) and soluble anti-CD28 (5 µg/ml) for 48 h before nucleofection. Electroporation was performed using the Amaxa P3 Primary Cell 96-well Nucleofector kit and 4D-Nucleofecter (Lonza). *Streptococcus pyogenes* Cas9 protein with a double nuclear localization tag at the C terminus was obtained from QB3 MacroLab (University of California, Berkeley, Berkeley, CA). CRISPR RNA (crRNA) for SIRT1 was designed to target all known isoforms and exons while avoiding single nucleotide polymorphisms, and the associated trans–activating crRNA (tracrRNA) were chemically synthesized (IDT). Mixed at a molar ratio of 1:1, crRNA and tracrRNA were incubated for 30 min at 37°C to generate 40 µM hybrids. An equal volume of 40 µM Cas9-NLS was carefully added to the duplexes and incubated for 15 min at 37°C, yielding a 20 µM Cas9–RNP complex mixture. For each reaction, $1–3 \times 10^5$ T cells were pelleted and resuspended in 20 µl P3 buffer (Lonza). 4 µl of 20 µM Cas9–RNP mix was added directly to these cells, and the entire volume was quickly transferred to the 96-well reaction cuvette. Cells were electroporated with the Amaxa 4D-Nucleofector (Lonza). Im-

mediately after nucleofection, 80 µl of prewarmed, complete RPMI was added to each reaction, and the cells were allowed to recover for 1 h at 37°C. Cells were then restimulated using the human T Cell Activation/Expansion kit (Miltenyi) and 80 U/ml of human IL-2.

Purification of recombinant SIRT1 protein

In short, 293T cells were transfected at 70–80% confluency with a Flag-SIRT1 vector using calcium phosphate. 48 h after transfection, cells were washed in PBS and harvested in CelLytic M buffer (Sigma-Aldrich) supplemented with HALT protease/phosphatase inhibitors (ThermoFisher) before affinity purification using the Flag M Purification kit (CELLMM2; Sigma-Aldrich) according to the manufacturer's instructions. Purified protein was kept in wash buffer (50 mM Tris and 150 mM NaCl) at −80°C until further use.

T cell nucleofection with recombinant SIRT1 protein

Approximately 3×10^5 resting CD8+ T cells and recombinant SIRT1 (1 µM final concentration) were mixed in 20 µl P3 buffer before quickly being transferred into a 96-well reaction cuvette (Amaxa P3 Primary Cell 96-well Nucleofector kit). Cells were electroporated as described under the T cell transduction . . . section and recovered in complete RPMI for 18 h before being processed for Western blotting.

Metabolic assays

OCR and ECAR were determined using a Seahorse XF96 Extracellular Flux Analyzer (Seahorse Bioscience). The instrument was a gift from the S.D. Bechtel, Jr. Foundation to the Gladstone Institutes. Resting or 3-h anti-CD3–activated T cells (5×10^5 per well) were seeded onto Cell-Tak–coated wells (354240; Corning) in nonbuffered RPMI 1640 medium (R1383; Sigma-Aldrich), glucose depleted or supplemented with 11 mM glucose and 2 mM sodium pyruvate. Measurements were obtained under basal conditions and after adding 1 µM oligomycin, 0.5 µM FCCP, 0.5 µM rotenone/antimycin A (103015-100; Seahorse Bioscience), and 2-deoxy-D-glucose (2-DG) at a final well concentration of 50 mM (Agilent Technologies). Lactate measurements were detected using the primary metabolism screen conducted by the West Coast Metabolomics Center. In brief, sorted T cell populations were treated with 1 µM oligomycin and harvested at various times (0, 15, and 60 min). Samples were run on a mass spectrometer (ALEX-CIS GC-TOF; GER STEL), and metabolites were quantified by peak heights and reported by retention index, quantification mass, biochemical database identifiers, and full mass spectra. Refer to Fiehn et al. (2008) for further details regarding data acquisition and processing.

Microarray and IPA

CD8+CD28+ and CD8+CD28− T cells were sorted from three human donors, and total RNA was extracted using the RNeasy Micro kit (Qiagen) according to the manufacturer's instructions. Microarray experiments were performed using the Affymetrix platform, and 159 significant genes were identified using a cutoff of ≥ 1.0 $\log_2$ fold change and ≤ 0.05 FDR (adjusted p-value). Using IPA software on the differentially expressed genes, a list of possible upstream regulators was generated based on the literature compiled in the Ingenuity Knowledge Base. Refer to the manufacturer's website (http://www.ingenuity.com) for further details. The complete array datasets can be viewed in the GEO database (accession no. GSE105150).

Cell viability

Using the alamarBlue Cell Viability Assay (88951; Thermo-Fisher), cells were incubated with alamarBlue reagent, and the percent reagent reduction was calculated according the manufacturer's instructions.

RNA extraction and qRT–PCR

Total RNA from samples was extracted using the RNeasy Plus Mini kit (74136; Qiagen). cDNA was generated using 50–500 ng of total RNA with Superscript III Reverse transcription (18080-044; ThermoFisher) and oligo(dT)$_{12-18}$ (18418-012; ThermoFisher). The SYBR green qPCR reactions contained 5 µl of 2× Maxima SYBR green/Rox qPCR Master Mix (K0221; ThermoFisher), 5 µl of diluted cDNA, and 1 nmol of both forward and reverse primers. The reactions were run using the following conditions: 50°C for 2 min and 95°C for 10 min, followed by 40 cycles of 95°C for 5 s and 60°C for 30 s. See Table S2 for a qRT-PCR primer list.

Western blot

Cells were lysed in radioimmunoprecipitation assay buffer (50 mM Tris-HCl, pH 8, 150 mM NaCl, 1% NP-40, 0.5% sodium deoxycholate, and 0.1% SDS, supplemented with protease inhibitor cocktail; Sigma-Aldrich) for 30 min at 4°C, or subcellular fractions were extracted using NE-PER Nuclear and Cytoplasmic Extraction Reagents (78835; ThermoFisher) according to the manufacturer's instructions. Samples were resuspended in Laemmli buffer for SDS-PAGE. For chemiluminescent detection, we used enhanced luminol-based chemiluminescent substrate (ECL) and ECL Hyperfilm (Amersham).

Antibodies

The following primary antibodies were used: SIRT1 (ab104833; Abcam; 8469S; Cell Signaling Technology), SIRT6 (12486; Cell Signaling Technology), SIRT7 (5360; Cell Signaling Technology), β-actin (A5316; Sigma-Aldrich), FoxO1 (2880S; Cell Signaling Technology), Sp1 (sc-14027; Santa Cruz), CD25-APC (17-0259-42; Affymetrix eBioscience), and CD69-APC (310910; BioLegend). For mass spectrometry analysis, a total anti-acetyllysine antibody was used (ICP0388-2MG; ImmuneChem).

Mass spectrometry analysis

Acetyllysine-containing peptides were enriched from cellular lysates as previously described (Downey et al., 2015). Analysis was performed in technical duplicates on an Orbitrap Fusion mass spectrometry system (Easy nLC 1200 ultra performance liquid chromatography with Nanospray Flex; ThermoFisher). Samples were injected on a C18 reverse phase column (25 cm × 75 µm packed with ReprosilPur C18 AQ 1.9-µm particles). Peptides were separated by an organic gradient from 5 to 30% acetonitrile in 0.1% formic acid over 120 min at a flow rate of 300 nl/min. The mass spectometer continuously acquired spectra in a data-dependent manner throughout the gradient, acquiring a full scan in the Orbitrap (at 120,000 resolution with an automatic gain control target of 200,000 and a maximum injection time of 100 ms), followed by as many tandem mass spectrometry scans as could be acquired on the most abundant ions in 3 s in the dual linear ion trap (rapid scan type with an intensity threshold of 5,000, higher-energy collisional dissociation energy of 29%, automatic gain control target of 10,000, a maximum injection time of 35 ms, and an isolation width of 1.6 m/z). Dynamic exclusion was enabled with a repeat count of 1, an exclusion duration of 20 s, and an exclusion mass width of ±10 ppm.

Raw mass spectrometry data were assigned to human protein sequences, and MS1 intensities were extracted with the MaxQuant software package (version 1.5.5.1; Cox and Mann, 2008). Data were searched against the SwissProt human protein database (downloaded on January 11, 2016). Variable modifications were allowed for N-terminal protein acetylation, methionine oxidation, and lysine acetylation. A static modification was indicated for carbamidomethyl cysteine. The Match between runs feature was enabled to match within 2 min between runs. All other settings were left using MaxQuant default settings.

Statistical analysis

Comparisons for two groups were calculated using a paired (comparing populations derived from the same donor) two-tailed Student's t test. Comparisons for more than two groups were calculated using one-way ANOVA, followed by Tukey's multiple comparison tests. Data are presented as mean ± SD for technical replicates or mean ± SEM for biological replicates. Statistical significance is indicated in all figures by the following annotations: *, $P < 0.05$; **, $P < 0.01$; ***, $P < 0.001$; ****, $P < 0.0001$.

Online supplemental material

Fig. S1 shows that the glycolytic capacity of resting CD8^{+}CD28^{−} T cells depends on glucose and SIRT1. Fig. S2 depicts the cytotoxicity and FoxO1 status in CD8^{+} T cell subsets. Fig. S3 shows that FoxO1 inhibitor increases GZMB expression without T cell activation. Table S1 presents a microarray that identified 159 differentially regulated genes between CD8^{+}CD28^{+} and CD8^{+}CD28^{−} T cells. Table S2 is a primer list for qRT-PCR.

REFERENCES

Amara, R.R., P. Nigam, S. Sharma, J. Liu, and V. Bostik. 2004. Long-lived poxvirus immunity, robust CD4 help, and better persistence of CD4 than CD8 T cells. *J. Virol.* 78:3811–3816. https://doi.org/10.1128/JVI.78.8.3811-3816.2004

Azuma, M., J.H. Phillips, and L.L. Lanier. 1993. CD28− T lymphocytes. Antigenic and functional properties. *J. Immunol.* 150:1147–1159.

Beier, U.H., L. Wang, T.R. Bhatti, Y. Liu, R. Han, G. Ge, and W.W. Hancock. 2011. Sirtuin-1 targeting promotes Foxp3+ T-regulatory cell function and prolongs allograft survival. *Mol. Cell. Biol.* 31:1022–1029. https://doi.org/10.1128/MCB.01206-10

Berdichevsky, A., M. Viswanathan, H.R. Horvitz, and L. Guarente. 2006. *C. elegans* SIR-2.1 interacts with 14-3-3 proteins to activate DAF-16 and extend life span. *Cell.* 125:1165–1177. https://doi.org/10.1016/j.cell.2006.04.036

Brunet, A., L.B. Sweeney, J.F. Sturgill, K.F. Chua, P.L. Greer, Y. Lin, H. Tran, S.E. Ross, R. Mostoslavsky, H.Y. Cohen, et al. 2004. Stress-dependent regulation of FOXO transcription factors by the SIRT1 deacetylase. *Science.* 303:2011–2015. https://doi.org/10.1126/science.1094637

Cantó, C., R.H. Houtkooper, E. Pirinen, D.Y. Youn, M.H. Oosterveer, Y. Cen, P.J. Fernandez-Marcos, H. Yamamoto, P.A. Andreux, P. Cettour-Rose, et al. 2012. The NAD(+) precursor nicotinamide riboside enhances oxidative metabolism and protects against high-fat diet-induced obesity. *Cell Metab.* 15:838–847. https://doi.org/10.1016/j.cmet.2012.04.022

Cham, C.M., G. Driessens, J.P. O'Keefe, and T.F. Gajewski. 2008. Glucose deprivation inhibits multiple key gene expression events and effector functions in CD8^{+} T cells. *Eur. J. Immunol.* 38:2438–2450. https://doi.org/10.1002/eji.200838289

Chang, H.C., and L. Guarente. 2014. SIRT1 and other sirtuins in metabolism. *Trends Endocrinol. Metab.* 25:138–145. https://doi.org/10.1016/j.tem.2013.12.001

Chang, C.H., J.D. Curtis, L.B. Maggi Jr., B. Faubert, A.V. Villarino, D. O'Sullivan, S.C. Huang, G.J. van der Windt, J. Blagih, J. Qiu, et al. 2013. Posttranscriptional control of T cell effector function by aerobic glycolysis. *Cell.* 153:1239–1251. https://doi.org/10.1016/j.cell.2013.05.016

Chen, G., A. Lustig, and N.-P. Weng. 2013. T cell aging: a review of the transcriptional changes determined from genome-wide analysis. *Front. Immunol.* 4:121. https://doi.org/10.3389/fimmu.2013.00121

Chiu, W.K., M. Fann, and N.P. Weng. 2006. Generation and growth of CD28[null]CD8^{+} memory T cells mediated by IL-15 and its induced cytokines. *J. Immunol.* 177:7802–7810. https://doi.org/10.4049/jimmunol.177.11.7802

Cho, S.-H., J.A. Chen, F. Sayed, M.E. Ward, F. Gao, T.A. Nguyen, G. Krabbe, P.D. Sohn, I. Lo, S. Minami, et al. 2015. SIRT1 deficiency in microglia contributes to cognitive decline in aging and neurodegeneration via epigenetic regulation of IL-1β. *J. Neurosci.* 35:807–818. https://doi.org/10.1523/JNEUROSCI.2939-14.2015

Cox, J., and M. Mann. 2008. MaxQuant enables high peptide identification rates, individualized p.p.b.-range mass accuracies and proteome-wide protein quantification. *Nat. Biotechnol.* 26:1367–1372. https://doi.org/10.1038/nbt.1511

Daitoku, H., M. Hatta, H. Matsuzaki, S. Aratani, T. Ohshima, M. Miyagishi, T. Nakajima, and A. Fukamizu. 2004. Silent information regulator 2 potentiates Foxo1-mediated transcription through its deacetylase activity. *Proc. Natl. Acad. Sci. USA.* 101:10042–10047. https://doi.org/10.1073/pnas.0400593101

Darrah, E., and A. Rosen. 2010. Granzyme B cleavage of autoantigens in autoimmunity. *Cell Death Differ.* 17:624–632. https://doi.org/10.1038/cdd.2009.197

Downey, M., J.R. Johnson, N.E. Davey, B.W. Newton, T.L. Johnson, S. Galaang, C.A. Seller, N. Krogan, and D.P. Toczyski. 2015. Acetylome profiling reveals overlap in the regulation of diverse processes by sirtuins, gcn5, and esa1. *Mol. Cell. Proteomics.* 14:162–176. https://doi.org/10.1074/mcp.M114.043141

Dutra, W.O., O.A. Martins-Filho, J.R. Cançado, J.C. Pinto-Dias, Z. Brener, G. Gazzinelli, J.F. Carvalho, and D.G. Colley. 1996. Chagasic patients lack CD28 expression on many of their circulating T lymphocytes. *Scand. J. Immunol.* 43:88–93. https://doi.org/10.1046/j.1365-3083.1996.d01-9.x

Effros, R.B. 2005. The role of CD8 T cell replicative senescence in human aging. *Discov. Med.* 5:293–297. https://doi.org/10.1111/j.0105-2896.2005.00259.x

Effros, R.B., N. Boucher, V. Porter, X. Zhu, C. Spaulding, R.L. Walford, M. Kronenberg, D. Cohen, and F. Schächter. 1994. Decline in CD28^{+} T cells in centenarians and in long-term T cell cultures: a possible cause for both in vivo and in vitro immunosenescence. *Exp. Gerontol.* 29:601–609. https://doi.org/10.1016/0531-5565(94)90073-6

Fagnoni, F.F., R. Vescovini, M. Mazzola, G. Bologna, E. Nigro, G. Lavagetto, C. Franceschi, M. Passeri, and P. Sansoni. 1996. Expansion of cytotoxic CD8^{+} CD28^{-} T cells in healthy ageing people, including centenarians. *Immunology.* 88:501–507. https://doi.org/10.1046/j.1365-2567.1996.d01-689.x

Fann, M., W.K. Chiu, W.H. Wood III, B.L. Levine, K.G. Becker, and N.-P. Weng. 2005. Gene expression characteristics of CD28[null] memory phenotype CD8^{+} T cells and its implication in T-cell aging. *Immunol. Rev.* 205:190–206. https://doi.org/10.1111/j.0105-2896.2005.00262.x

Fiehn, O., G. Wohlgemuth, M. Scholz, T. Kind, D.Y. Lee, Y. Lu, S. Moon, and B. Nikolau. 2008. Quality control for plant metabolomics: reporting MSI-compliant studies. *Plant J.* 53:691–704. https://doi.org/10.1111/j.1365-313X.2007.03387.x

Frescas, D., L. Valenti, and D. Accili. 2005. Nuclear trapping of the forkhead transcription factor FoxO1 via Sirt-dependent deacetylation promotes expression of glucogenetic genes. *J. Biol. Chem.* 280:20589–20595. https://doi.org/10.1074/jbc.M412357200

Gong, H., J. Pang, Y. Han, Y. Dai, D. Dai, J. Cai, and T.-M. Zhang. 2014. Age-dependent tissue expression patterns of Sirt1 in senescence-accelerated mice. *Mol. Med. Rep.* 10:3296–3302. https://doi.org/10.3892/mmr.2014.2648

Gross, D.N., A.P.J. van den Heuvel, and M.J. Birnbaum. 2008. The role of FoxO in the regulation of metabolism. *Oncogene.* 27:2320–2336. https://doi.org/10.1038/onc.2008.25

Guarente, L. 2011. Franklin H. Epstein Lecture: Sirtuins, aging, and medicine. *N. Engl. J. Med.* 364:2235–2244. https://doi.org/10.1056/NEJMra1100831

Gubser, P.M., G.R. Bantug, L. Razik, M. Fischer, S. Dimeloe, G. Hoenger, B. Durovic, A. Jauch, and C. Hess. 2013. Rapid effector function of memory CD8^{+} T cells requires an immediate-early glycolytic switch. *Nat. Immunol.* 14:1064–1072. https://doi.org/10.1038/ni.2687

Hall, J.A., J.E. Dominy, Y. Lee, and P. Puigserver. 2013. The sirtuin family's role in aging and age-associated pathologies. *J. Clin. Invest.* 123:973–979. https://doi.org/10.1172/JCI64094

Hamann, D., P.A. Baars, M.H. Rep, B. Hooibrink, S.R. Kerkhof-Garde, M.R. Klein, and R.A. van Lier. 1997. Phenotypic and functional separation of memory and effector human CD8+ T cells. *J. Exp. Med.* 186:1407–1418. https://doi.org/10.1084/jem.186.9.1407

Henson, S.M., O. Franzese, R. Macaulay, V. Libri, R.I. Azevedo, S. Kiani-Alikhan, F.J. Plunkett, J.E. Masters, S. Jackson, S.J. Griffiths, et al. 2009. KLRG1 signaling induces defective Akt (ser473) phosphorylation and proliferative dysfunction of highly differentiated CD8^{+} T cells. *Blood.* 113:6619–6628. https://doi.org/10.1182/blood-2009-01-199588

Henson, S.M., A. Lanna, N.E. Riddell, O. Franzese, R. Macaulay, S.J. Griffiths, D.J. Puleston, A.S. Watson, A.K. Simon, S.A. Tooze, and A.N. Akbar. 2014. p38 signaling inhibits mTORC1-independent autophagy in senescent human CD8^{+} T cells. *J. Clin. Invest.* 124:4004–4016. https://doi.org/10.1172/JCI75051

Hiebert, P.R., and D.J. Granville. 2012. Granzyme B in injury, inflammation, and repair. *Trends Mol. Med.* 18:732–741. https://doi.org/10.1016/j.molmed.2012.09.009

Houtkooper, R.H., E. Pirinen, and J. Auwerx. 2012. Sirtuins as regulators of metabolism and healthspan. *Nat. Rev. Mol. Cell Biol.* 13:225–238. https://doi.org/10.1038/nrm3293

Hubbard, B.P., A.P. Gomes, H. Dai, J. Li, A.W. Case, T. Considine, T.V. Riera, J.E. Lee, S.Y. e, D.W. Lamming, et al. 2013. Evidence for a common mechanism of SIRT1 regulation by allosteric activators. *Science.* 339:1216–1219. https://doi.org/10.1126/science.1231097

Hultquist, J.F., K. Schumann, J.M. Woo, L. Manganaro, M.J. McGregor, J. Doudna, V. Simon, N.J. Krogan, and A. Marson. 2016. A Cas9 Ribonucleoprotein Platform for Functional Genetic Studies of HIV-Host Interactions in Primary Human T Cells. *Cell Reports.* 17:1438–1452. https://doi.org/10.1016/j.celrep.2016.09.080

Jenwitheesuk, A., P. Boontem, P. Wongchitrat, J. Tocharus, S. Mukda, and P. Govitrapong. 2017. Melatonin regulates the aging mouse hippocampal homeostasis via the sirtuin1-FOXO1 pathway. *EXCLI J.* 16:340–353. https://doi.org/10.17179/excli2016-852

Jin, F., Q. Wu, Y.-F. Lu, Q.-H. Gong, and J.-S. Shi. 2008. Neuroprotective effect of resveratrol on 6-OHDA–induced Parkinson's disease in rats. *Eur. J. Pharmacol.* 600:78–82. https://doi.org/10.1016/j.ejphar.2008.10.005

Joshi, N.S., W. Cui, A. Chandele, H.K. Lee, D.R. Urso, J. Hagman, L. Gapin, and S.M. Kaech. 2007. Inflammation directs memory precursor and short-lived effector CD8([+]) T cell fates via the graded expression of T-bet transcription factor. *Immunity.* 27:281–295. https://doi.org/10.1016/j.immuni.2007.07.010

Kaeberlein, M., M. McVey, and L. Guarente. 1999. The SIR2/3/4 complex and SIR2 alone promote longevity in *Saccharomyces cerevisiae* by two different mechanisms. *Genes Dev.* 13:2570–2580. https://doi.org/10.1101/gad.13.19.2570

Kerdiles, Y.M., D.R. Beisner, R. Tinoco, A.S. Dejean, D.H. Castrillon, R.A. DePinho, and S.M. Hedrick. 2009. Foxo1 links homing and survival of naive T cells by regulating L-selectin, CCR7 and interleukin 7 receptor. *Nat. Immunol.* 10:176–184. https://doi.org/10.1038/ni.1689

Kerdiles, Y.M., E.L. Stone, D.R. Beisner, M.A. McGargill, I.L. Ch'en, C. Stockmann, C.D. Katayama, and S.M. Hedrick. 2010. Foxo transcription factors control regulatory T cell development and function. *Immunity*. 33:890–904. https://doi.org/10.1016/j.immuni.2010.12.002

Kim, M.V., W. Ouyang, W. Liao, M.Q. Zhang, and M.O. Li. 2013. The transcription factor Foxo1 controls central-memory CD8^{+} T cell responses to infection. *Immunity*. 39:286–297. https://doi.org/10.1016/j.immuni.2013.07.013

Kuroda, S., M. Yamazaki, M. Abe, K. Sakimura, H. Takayanagi, and Y. Iwai. 2011. Basic leucine zipper transcription factor, ATF-like (BATF) regulates epigenetically and energetically effector CD8 T-cell differentiation via Sirt1 expression. *Proc. Natl. Acad. Sci. USA*. 108:14885–14889. https://doi.org/10.1073/pnas.1105133108

Kwon, H.-S., H.W. Lim, J. Wu, M. Schnölzer, E. Verdin, and M. Ott. 2012. Three novel acetylation sites in the Foxp3 transcription factor regulate the suppressive activity of regulatory T cells. *J. Immunol*. 188:2712–2721. https://doi.org/10.4049/jimmunol.1100903

Lee, D., and A.L. Goldberg. 2013. SIRT1 protein, by blocking the activities of transcription factors FoxO1 and FoxO3, inhibits muscle atrophy and promotes muscle growth. *J. Biol. Chem*. 288:30515–30526. https://doi.org/10.1074/jbc.M113.489716

Lim, H.W., S.G. Kang, J.K. Ryu, B. Schilling, M. Fei, I.S. Lee, A. Kehasse, K. Shirakawa, M. Yokoyama, M. Schnölzer, et al. 2015. SIRT1 deacetylates RORγt and enhances Th17 cell generation. *J. Exp. Med*. 212:607–617. https://doi.org/10.1084/jem.20132378

Lin, K., J.B. Dorman, A. Rodan, and C. Kenyon. 1997. daf-16: An HNF-3/forkhead family member that can function to double the life-span of *Caenorhabditis elegans*. *Science*. 278:1319–1322. https://doi.org/10.1126/science.278.5341.1319

Man, K., and A. Kallies. 2015. Synchronizing transcriptional control of T cell metabolism and function. *Nat. Rev. Immunol*. 15:574–584. https://doi.org/10.1038/nri3874

Matsuzaki, H., H. Daitoku, M. Hatta, H. Aoyama, K. Yoshimochi, and A. Fukamizu. 2005. Acetylation of Foxo1 alters its DNA-binding ability and sensitivity to phosphorylation. *Proc. Natl. Acad. Sci. USA*. 102:11278–11283. https://doi.org/10.1073/pnas.0502738102

Michelini, R.H, A.L. Doedens, A.W. Goldrath, and S.M. Hedrick. 2013. Differentiation of CD8 memory T cells depends on Foxo1. *J. Exp. Med*. 210:1189–1200. https://doi.org/10.1084/jem.20130392

Miller, J.D., R.G. van der Most, R.S. Akondy, J.T. Glidewell, S. Albott, D. Masopust, K. Murali-Krishna, P.L. Mahar, S. Edupuganti, S. Lalor, et al. 2008. Human effector and memory CD8^{+} T cell responses to smallpox and yellow fever vaccines. *Immunity*. 28:710–722. https://doi.org/10.1016/j.immuni.2008.02.020

Motta, M.C., N. Divecha, M. Lemieux, C. Kamel, D. Chen, W. Gu, Y. Bultsma, M. McBurney, and L. Guarente. 2004. Mammalian SIRT1 represses forkhead transcription factors. *Cell*. 116:551–563. https://doi.org/10.1016/S0092-8674(04)00126-6

Nagashima, T., N. Shigematsu, R. Maruki, Y. Urano, H. Tanaka, A. Shimaya, T. Shimokawa, and M. Shibasaki. 2010. Discovery of novel forkhead box O1 inhibitors for treating type 2 diabetes: improvement of fasting glycemia in diabetic db/db mice. *Mol. Pharmacol*. 78:961–970. https://doi.org/10.1124/mol.110.065714

Ouyang, W., O. Beckett, R.A. Flavell, and M.O. Li. 2009. An essential role of the Forkhead-box transcription factor Foxo1 in control of T cell homeostasis and tolerance. *Immunity*. 30:358–371. https://doi.org/10.1016/j.immuni.2009.02.003

Park, R.J., T. Wang, D. Koundakjian, J.F. Hultquist, P. Lamothe-Molina, B. Monel, K. Schumann, H. Yu, K.M. Krupczak, W. Garcia-Beltran, et al. 2017. A genome-wide CRISPR screen identifies a restricted set of HIV host dependency factors. *Nat. Genet*. 49:193–203. https://doi.org/10.1038/ng.3741

Pearce, E.L., M.C. Poffenberger, C.H. Chang, and R.G. Jones. 2013. Fueling immunity: insights into metabolism and lymphocyte function. *Science*. 342:1242454. https://doi.org/10.1126/science.1242454

Posnett, D.N., R. Sinha, S. Kabak, and C. Russo. 1994. Clonal populations of T cells in normal elderly humans: the T cell equivalent to "benign monoclonal gammapathy". *J. Exp. Med*. 179:609–618. https://doi.org/10.1084/jem.179.2.609

Quintas, A., A.J. de Solís, F.J. Díez-Guerra, J.M. Carrascosa, and E. Bogónez. 2012. Age-associated decrease of SIRT1 expression in rat hippocampus: prevention by late onset caloric restriction. *Exp. Gerontol*. 47:198–201. https://doi.org/10.1016/j.exger.2011.11.010

Rao, R.R., Q. Li, M.R. Gubbels Bupp, and P.A. Shrikant. 2012. Transcription factor Foxo1 represses T-bet-mediated effector functions and promotes memory CD8([+]) T cell differentiation. *Immunity*. 36:374–387. https://doi.org/10.1016/j.immuni.2012.01.015

Sack, M.N., and T. Finkel. 2012. Mitochondrial metabolism, sirtuins, and aging. *Cold Spring Harb. Perspect. Biol*. 4:a013102. https://doi.org/10.1101/cshperspect.a013102

Sallusto, F., D. Lenig, R. Förster, M. Lipp, and A. Lanzavecchia. 1999. Two subsets of memory T lymphocytes with distinct homing potentials and effector functions. *Nature*. 401:708–712. https://doi.org/10.1038/44385

Saukkonen, J.J., H. Kornfeld, and J.S. Berman. 1993. Expansion of a CD8^{+}CD28^{–} cell population in the blood and lung of HIV-positive patients. *J. Acquir. Immune Defic. Syndr*. 6:1194–1204.

Schumann, K., S. Lin, E. Boyer, D.R. Simeonov, M. Subramaniam, R.E. Gate, G.E. Haliburton, C.J. Ye, J.A. Bluestone, J.A. Doudna, and A. Marson. 2015. Generation of knock-in primary human T cells using Cas9 ribonucleoproteins. *Proc. Natl. Acad. Sci. USA*. 112:10437–10442. https://doi.org/10.1073/pnas.1512503112

Sin, T.K., A.P. Yu, B.Y. Yung, S.P. Yip, L.W. Chan, C.S. Wong, M. Ying, J.A. Rudd, and P.M. Siu. 2014. Modulating effect of SIRT1 activation induced by resveratrol on Foxo1-associated apoptotic signalling in senescent heart. *J. Physiol*. 592:2535–2548. https://doi.org/10.1113/jphysiol.2014.271387

Sin, T.K., B.Y. Yung, and P.M. Siu. 2015. Modulation of SIRT1-Foxo1 signaling axis by resveratrol: implications in skeletal muscle aging and insulin resistance. *Cell. Physiol. Biochem*. 35:541–552. https://doi.org/10.1159/000369718

Staron, M.M., S.M. Gray, H.D. Marshall, I.A. Parish, J.H. Chen, C.J. Perry, G. Cui, M.O. Li, and S.M. Kaech. 2014. The transcription factor FoxO1 sustains expression of the inhibitory receptor PD-1 and survival of antiviral CD8(+) T cells during chronic infection. *Immunity*. 41:802–814. https://doi.org/10.1016/j.immuni.2014.10.013

Sun, Z., W. Zhong, X. Lu, B. Shi, Y. Zhu, L. Chen, G. Zhang, and X. Zhang. 2008. Association of Graves' disease and prevalence of circulating IFN-γ-producing CD28- T cells. *J. Clin. Immunol*. 28:464–472. https://doi.org/10.1007/s10875-008-9213-4

Tanno, M., A. Kuno, T. Yano, T. Miura, S. Hisahara, S. Ishikawa, K. Shimamoto, and Y. Horio. 2010. Induction of manganese superoxide dismutase by nuclear translocation and activation of SIRT1 promotes cell survival in chronic heart failure. *J. Biol. Chem*. 285:8375–8382. https://doi.org/10.1074/jbc.M109.090266

Tarazona, R., O. DelaRosa, C. Alonso, B. Ostos, J. Espejo, J. Peña, and R. Solana. 2001. Increased expression of NK cell markers on T lymphocytes in aging and chronic activation of the immune system reflects the accumulation of effector/senescent T cells. *Mech. Ageing Dev*. 121:77–88. https://doi.org/10.1016/S0047-6374(00)00199-8

Tissenbaum, H.A., and L. Guarente. 2001. Increased dosage of a sir-2 gene extends lifespan in *Caenorhabditis elegans*. *Nature*. 410:227–230. https://doi.org/10.1038/35065638

Vallejo, A.N. 2005. CD28 extinction in human T cells: altered functions and the program of T-cell senescence. *Immunol. Rev*. 205:158–169. https://doi.org/10.1111/j.0105-2896.2005.00256.x

van Loosdregt, J., Y. Vercoulen, T. Guichelaar, Y.Y.J. Gent, J.M. Beekman, O. van Beekum, A.B. Brenkman, D.-J. Hijnen, T. Mutis, E. Kalkhoven, et al. 2010. Regulation of Treg functionality by acetylation-mediated Foxp3 protein stabilization. *Blood*. 115:965–974. https://doi.org/10.1182/blood-2009-02-207118

Weng, N.-P., A.N. Akbar, and J. Goronzy. 2009. CD28(-) T cells: their role in the age-associated decline of immune function. *Trends Immunol*. 30:306–312. https://doi.org/10.1016/j.it.2009.03.013

Wertheimer, A.M., M.S. Bennett, B. Park, J.L. Uhrlaub, C. Martinez, V. Pulko, N.L. Currier, D. Nikolich-Žugich, J. Kaye, and J. Nikolich-Žugich. 2014. Aging and cytomegalovirus infection differentially and jointly affect distinct circulating T cell subsets in humans. *J. Immunol*. 192:2143–2155. https://doi.org/10.4049/jimmunol.1301721

Zhang, H., D. Ryu, Y. Wu, K. Gariani, X. Wang, P. Luan, D. D'Amico, E.R. Ropelle, M.P. Lutolf, R. Aebersold, et al. 2016. NAD$^+$ repletion improves mitochondrial and stem cell function and enhances life span in mice. *Science*. 352:1436–1443. https://doi.org/10.1126/science.aaf2693